value computed with the k-ε model is 1.5. This small disagreement is also seen in the flow redevelopment region downstream of the reattachment (X/D = 1.73). The algebraic turbulence models predict the reattachment point better than the k-ε model. The velocity profiles predicted with these algebraic models are in fairly good agreement with the experimentally obtained profiles at these two stations. The Chow model predictions are slightly better than those of the Baldwin-Lomax model in this flow redevelopment region. The vertical (w) component of the velocity is better predicted by the k-ε model than it is by the algebraic models both in the flow recirculation and redevelopment regions. The profiles made by the algebraic models are in especially poor agreement with the experimental data for radial positions greater than half of the base radius. Figure 2c shows the turbulent shear stress profiles in the wake. The computed values obtained by both the algebraic models and the k-ε model are compared with the experimental data. In general, a small improvement can be observed in the values predicted with the k-ε model over those predicted with the algebraic models. A discrepancy exists between the experimentally obtained turbulent shear stress and the predicted shear stresses with all of the turbulence models. This is especially true near the peaks at X/D = 1.26 and 1.42. The magnitude of the peak predicted by the k-ε model is about the same as that predicted by the Baldwin-Lomax model at these two positions; however, they both underpredict the experimental peak. The Chow model underpredicts the peak even more. As for the location of the peak, the k-ε model does better than the algebraic models. As X/D is increased from 1.26 to 1.42, the location of the peak predicted by the k-ε model shifts downward and moves closer to the center line similar to that observed in the experiment. This is not seen in the predictions made by the algebraic models. The k-ε model prediction agrees better than the predictions made by the algebraic models at X/D = 1.73.

Of particular interest is the accurate prediction or determination of base pressure and, hence, base drag. Figure 3 shows the base pressure distribution (over the base). The base pressures predicted by both the algebraic models and the two-equation k-ε turbulence model are compared with the experimental data. The experimental data are shown in dark circles and the computed results are shown in lines. The base pressures predicted by both algebraic turbulence models show a big increase near the center line of symmetry. The experimental data shows almost no change (only 3%) in the base pressure distribution. The base pressures are very poorly predicted by the algebraic models, not only near the center line but also near the base corner. A much-improved base pressure distribution is predicted by the k-ε model and its agreement with the measured base pressure is quite good. As expected, the k-ε prediction shows a small increase in the base pressure near the center line; however, it is unclear why it is not observed in the data. The average base pressure computed by the k-ε model is within 5% of the experimental value whereas the algebraic models predictions differ from the experimental value by 20–25%. Detailed analysis of the near wake flowfields and the eddy viscosities computed by these models reveal significant differences in the eddy viscosity in the free mixing shear layer region ($r/R \approx 0.4$–0.6) and the reverse velocity in the near wake near the centerline. In the shear layer where the velocity gradients are large, the algebraic models predict large eddy viscosities whereas the k-ε model predicts small values. This difference in the mixing region results in small reverse velocities in the near wake with the k-ε model and large reverse velocities with the algebraic models. This in turn results in higher stagnation pressure at the base at the centerline and a large variation of base pressure over the base. With the k-ε model, small reverse velocities in the centerline near the base result in only a small increase in the pressure as the flow stagnates and subsequently to a flatter pressure variation over the base. The k-ε computations generally required 50% more computational time than the algebraic model predictions.

Conclusions

A zonal, implicit, time-marching Navier-Stokes computational technique has been used to compute the turbulent supersonic base flow over a cylindrical afterbody. Flowfield computations have been performed at M_∞ = 2.46 using two algebraic models and a two-equation k-ε turbulence model.

Comparison of both the mean and turbulence quantities have been made with the available experimental data. Both algebraic turbulence models predict the mean velocity components poorly in the recirculatory flow region in the wake. In general, the velocity components predicted by the two-equation k-ε model are in better agreement with the experimental data than those predicted by the algebraic models. Computed base pressure distributions have been compared with the measured base pressures. The base pressures predicted by the algebraic models show a much larger variation and are in worse agreement with the data. The measured base pressures show a very small change along the base and are predicted rather well with the k-ε turbulence model.

References

[1]Sahu, J., Nietubicz, C. J., and Steger, J. L., "Navier-Stokes Computations of Projectile Base Flow With and Without Base Injection," *AIAA Journal*, Vol. 23, No. 9, 1985, pp. 1348–1355.

[2]Herrin, J. L., and Dutton, J. C., "An Experimental Investigation of the Supersonic Axisymmetric Base Flow Behind a Cylindrical Afterbody," Univ. of Illinois at Urbana-Champaign, UILU 91-4004, Urbana, IL, May 1991.

[3]Baldwin, B. S., and Lomax, H., "Thin-Layer Approximation and Algebraic Model for Separated Turbulent Flows," AIAA Paper 78-257, Jan. 1978.

[4]Chow, W. L., "Improvement on Numerical Computation of the Thin-Layer Navier-Stokes Equation—With Special Emphasis on the Turbulent Base Pressure of a Projectile in Transonic Flight Condition," Univ. of Illinois at Urbana-Champaign, CR No. DAAG29-81-D-0100, Urbana, IL, Nov. 1985.

[5]Chien, K. Y., "Predictions of Channel and Boundary-Layer Flows with a Low-Reynolds-Number Turbulence Model," *AIAA Journal*, Vol. 20, No. 1, 1982, pp. 33–38.

Demonstration of an Elastically Coupled Twist Control Concept for Tilt Rotor Blade Application

R. C. Lake,* M. W. Nixon,† M. L. Wilbur,*
J. D. Singleton,* and P. H. Mirick†
NASA Langley Research Center,
Hampton, Virginia 23681

Introduction

GIVEN the complex, directional nature of composite materials, as well as the complicated structural design requirements associated with advanced tilt rotor blade designs, many problems arise in the development of extension-twist-coupled tilt rotor blades. Foremost among these is the lack of an extensive analytical/experimental database for elastically coupled structures. As such, significant amounts of basic research directed toward developing a better understanding of the fundamental problems inherent in new design concepts are required. For example, the effects of pretwist on the extension, bending, and torsional behavior of anisotropic beams with nonhomogeneous, irregular cross sections were investigated in Ref. 1. Numerical results indicated that the torsional stiffness in the one- and two-cell designs varied as a function of pretwist magnitude, decreasing for moderate levels of pretwist while increasing for high pretwist levels, when the

Presented as Paper 92-2468 at the AIAA/ASME/ASCE/AHS/ASC 33rd Structures, Structural Dynamics, and Materials Conference, Dallas, TX, April 13–15, 1992; received July 11, 1992; revision received Aug. 11, 1993; accepted for publication Oct. 26, 1993.

*Research engineer, MS 340. Member AIAA.
†Research engineer, MS 340.

pretwist axis was held at the section centroid. Varying the location of the pretwist axis affected the magnitude and directional nature of the extension-twist coupling such that the beam would untwist or further twist in response to an applied extension. Additional problems associated with the design of practical extension-twist-coupled rotor blades include the determination of optimum twist distributions that may be realistically obtained from current composite material systems, such as that studied in Ref. 2. Test data obtained from static tensile and torsion tests conducted on a set of extension-twist-coupled circular tube designs verified that the twist deformation required for tilt rotor blade designs could be achieved using a $([+20/-70\ \text{deg}]_2)_s$ laminate design. This study was further expanded in Ref. 3, where a set of extension-twist-coupled tilt rotor blade designs with varying amounts of tip weight was developed to achieve maximum twist deformations within material design limits. Maximum twist deformations of 19 and 27.3 deg were analytically obtained for the 0–100% rpm range for two practical designs, resulting in twist deformations between 80–100% rpm of 6.9 and 9.8 deg, respectively. Although these results indicate that passive blade twist control is viable and can enhance current tilt rotor blade performance, an experimental verification of the concept is a necessary prerequisite in the practical development of an extension-twist-coupled tilt rotor blade design.

The purpose of this Note is to present results from an analytical/experimental study that investigated the potential for passively changing blade twist through the use of extension-twist coupling. A set of composite model rotor blades was manufactured from existing blade molds for a low-twist metal helicopter rotor blade, with a view toward establishing a preliminary "proof of concept" for extension-twist-coupled rotor blades. Data were obtained in hover for both a ballasted and unballasted blade configuration in sea-level atmospheric conditions. Test data were compared with results obtained from a geometrically nonlinear analysis of a detailed finite element model of the rotor blade developed in MSC/NASTRAN.

Apparatus and Procedures

Model Description

A four-bladed articulated model rotor hub with coincident lead-lag and flapping hinges was used in this investigation. A set of composite model rotor blades, manufactured from existing blade molds for a low-twist helicopter rotor blade, was tested during this investigation. These blades were rectangular in planform with an initial twist θ_1 of -8.25 deg (nose down) with zero twist initiating at the blade root and decreasing linearly along the blade span. The rotor diameter measured 110 in. tip to tip and had a solidity of 0.0982. The cross section of the extension-twist-coupled model rotor blade is shown in Fig. 1. The spar incorporated a NACA 0012 airfoil design and was fabricated using four plies of Fiberite graphite/epoxy in a plain weave cloth "pre-preg." The 0/90-deg cloth weave was rotated off-axis to achieve a $([+20\ \text{deg}]_4)$ extension-twist-coupled laminate. Two hollow fiberglass weight tubes were incorporated into the blade design to provide a means of changing the nonstructural mass distribution. The tubes spanned the full length of the blade (42.5 in.) and were located immediately fore and aft of the blade spar and centered about the quarter-chord. Two different mass distributions were used in this study to produce different levels of centrifugal force and thus blade twist: a ballasted configuration (2.60 lb total) in which both weight tubes were filled with tungsten weights and an unballasted configuration (1.44 lb total) in which both weight tubes remained empty. The geometric properties of the extension-twist-coupled model rotor blades, as well as the material properties, weights, and inertias, are specified in Ref. 4.

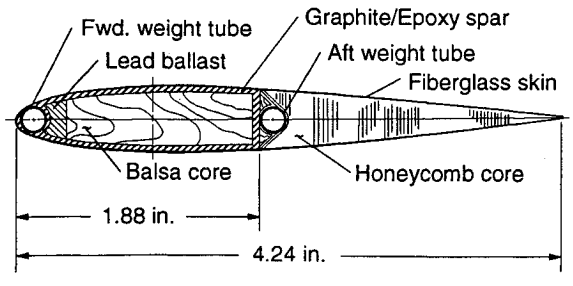

Fig. 1 Extension-twist-coupled rotor blade cross section.

Two blades were instrumented with a set of four resistance-wire Wheatstone bridge strain gauges located on the upper and lower surfaces of each blade at radial stations 20.75, 29.45, 41.00, and 47.05. These gauges were calibrated to bending moments in the flap and chord directions and to twist in the torsion direction. The bending moments were used to monitor blade structural integrity during the test, whereas the twist function was used to measure the change in blade elastic twist as a function of rotor speed. The set of blades was tested using the Aeroelastic Rotor Experimental System (ARES) model.

Test Procedure

The experimental investigation was conducted in the Helicopter Hover Facility (HHF) and the Transonic Dynamics Tunnel (TDT) located at NASA Langley. For this investigation, air at atmospheric pressure (with a density of 0.00234 slugs/ft^3) was used as the test medium in a "wind-off" condition. The change in blade elastic twist as a function of rotor speed was demonstrated by spinning the rotor blades in an atmospheric hover condition for both an unballasted and ballasted blade configuration. The blades were spun through the 0–800 rpm range at 100 rpm intervals using a shaft angle of attack of 0 deg. At each rpm interval, a corresponding sweep of collective pitch angle θ was performed to determine the effect of increased lift on the blade elastic twist. The initial collective pitch angle for each rpm interval was set to the minimum necessary to obtain a zero coning condition for the blades. Data were averaged and recorded for this condition. The collective pitch was then varied in increments of 2 deg up to a maximum pitch of 18 deg, and data were recorded at each corresponding value of collective pitch.

Analysis Model

The composite rotor blade was modeled and analyzed using the MSC/NASTRAN finite element program.[5] Flat plate elements were used to represent the composite spar laminate and skin, whereas solid elements were used to model the balsa wood and honeycomb filler components internal to the blade structure. Beam elements were used to represent the two internal ballast weight tubes within the blade as well as the transition blade area, root anchor, rotor cuff, and hub arm. The finite element model was analyzed for a collective pitch setting of 0 deg, measured at the blade root. Further details regarding the finite element model can be found in Ref. 4.

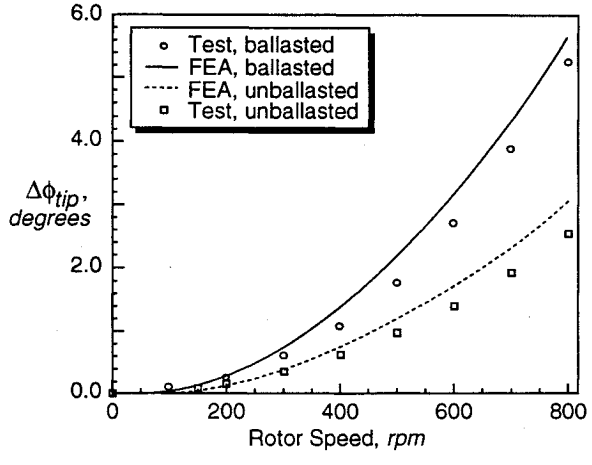

Fig. 2 Change in blade elastic twist at tip as a function of rotor speed.

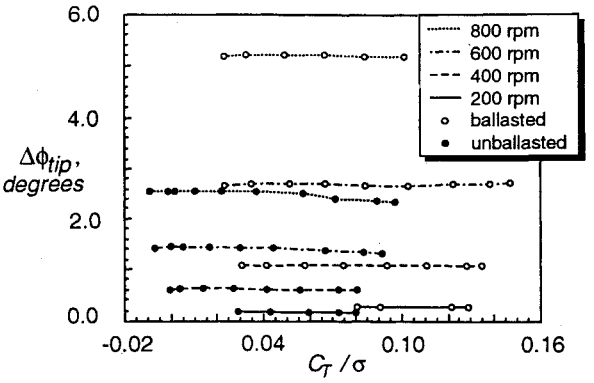

Fig. 3 Change in blade elastic twist at tip as a function of thrust coefficient-solidity ratio.

Discussion of Results

A set of extension-twist-coupled composite model rotor blades was tested as previously described. The change in blade elastic twist, $\Delta\phi_{tip}$ (positive nose up) is plotted as a function of rotor speed for test and analysis, using both mass distributions, in Fig. 2. The data points represent twist values recorded for the lowest available collective pitch settings at each rpm interval. Test results showed maximum twists of 2.54 deg for the unballasted blade configuration and 5.24 deg for the ballasted blade. These results were compared with a geometrically nonlinear finite element analysis that yielded maximum twists of 3.02 deg for the unballasted blade configuration and 5.61 deg for the ballasted blade configuration.

The effect of blade collective pitch on the blade elastic twist is shown in Fig. 3 for both blade configurations. The change in blade elastic twist is plotted as a function of the thrust coefficient-solidity ratio C_T/σ. Typically, an increase in collective blade pitch results in increased thrust, which causes the blades to flap upward. The magnitude of this flap angle, if significant, could decrease the effective centrifugal force acting on the blade, thereby decreasing the magnitude of twist obtained. However, no appreciable degradation in the blade elastic twist was observed for either configuration because the blade coning angle remained small throughout the sweep, reaching a maximum of only 2.5 deg during the ballasted configuration test run.

Although the total change in twist achieved in this preliminary study (5.24 deg over 0–100% rotor speed) indicates that passive blade twist control is feasible, significantly larger twist changes are required for practical tilt rotor blade designs. As indicated in Ref. 3, this goal can be realistically achieved by decreasing torsional stiffness and including blade tip weight (features not exploited in this study) in an extension-twist-coupled blade design.

Conclusions

This study has demonstrated the feasibility of passive blade twist control for composite rotor blades. Hover testing of the set of blades produced maximum twist changes of 2.54 deg for the unballasted blade configuration and 5.24 deg for the ballasted blade configuration. These results compared well with those obtained from a detailed finite element analysis model of the rotor blade, which yielded maximum twists of 3.02 and 5.61 deg for the unballasted and ballasted blade configurations, respectively. The effect of collective pitch sweep on the blade elastic twist was also demonstrated to be minimal, since no appreciable degradation in twist was observed at increased collective pitch angles. Results from this study provide a basis for the design of a highly twisted extension-twist-coupled model blade for tilt rotor aircraft by demonstrating the potential for improved dynamic and aerodynamic characteristics.

References

[1]Kosmatka, J. B., "Extension-Bend-Twist Coupling Behavior of Nonhomogeneous Anisotropic Beams with Initial Twist," *Proceedings of the AIAA/ASME/ASCE/AHS/ASC 32nd Structures, Structural Dynamics, and Materials Conference* (Baltimore, MD), AIAA, Washington, DC, 1991, pp. 1462–1474.

[2]Nixon, M. W., "Extension-Twist Coupling of Composite Circular Tubes with Application to Tilt Rotor Blade Design," *Proceedings of the AIAA/ASME/ASCE/AHS 28th Structures, Structural Dynamics, and Materials Conference* (Monterey, CA), AIAA, New York, 1987, pp. 295–303.

[3]Nixon, M. W., "Improvements to Tilt Rotor Performance Through Passive Blade Twist Control," NASA TM-100583, AVSCOM TM-88-B-010, April 1988.

[4]Lake, R. C., Nixon, M. W., Wilbur, M. W., Singleton, J. D., and Mirick, P. H., "A Demonstration of Passive Blade Twist Control Using Extension-Twist Coupling," *Proceedings of the AIAA/ASME/ASCE/AHS/ASC 33rd Structures, Structural Dynamics, and Materials Conference* (Dallas, TX), AIAA, Washington, DC, 1992, pp. 774–781.

[5]*MSC/NASTRAN User's Manual—Version 64*, MacNeal-Schwendler Corp., MSR-39, Los Angeles, CA, July 1984.

Contribution of the Truncated Modes to Eigenvector Derivatives

Zhong-sheng Liu*
Peking University, Beijing 100871, People's Republic of China
Su-huan Chen†
Jilin University of Technology, Changchun 130022, People's Republic of China
Min Yu‡
Peking University, Beijing 100871, People's Republic of China
and
You-qun Zhao‡
Jilin University of Technology, Changchun 130022, People's Republic of China

I. Introduction

THE usefulness of modal sensitivities for analysis and design of structural systems is well known. Some specific applications include redesign of vibratory systems and design of control systems by pole placement. Therefore, methods of computing eigenvector derivatives have been an active area of research since the work of Fox and Kapoor.[1] Recent development in this area was surveyed by Haftka and Adelman.[2] Basically, there are two methods for computing eigenvector derivatives: algebraic methods and modal superposition methods. Algebraic methods using only the eigenvector of concern are available in Refs. 1 and 3. Since algebraic methods require special manipulation of the system matrix for each eigenvector of concern, they can not be implemented easily and are not efficient if a large number of eigenvector derivatives are required. To obtain exact solutions, Nelson's method[3] is the most efficient of the algebraic methods if few eigenvector derivatives are required. However, when many eigenvector derivatives are required, modal superposition methods are more efficient. Because of the cost of generating computer solutions for a dynamic analysis, it is often impractical to obtain all modes. Therefore, only the first low-frequency modes are computed and are used as basis vectors of eigenvector derivatives. However, modal truncation induces errors which can be significant if more high-frequency modes are truncated. An explicit method to improve the truncated modal superposition representation of eigenvector derivatives is presented in Ref. 4, in which a residual static mode is used to approximate the contribution due to unavailable high-frequency modes. The numerical performance of the cited methods is compared in Ref. 5.

Received May 30, 1992; revision received Oct. 24, 1993; accepted for publication Oct. 24, 1993.

*Associate Professor, Department of Mechanics.
†Professor, Department of Mechanics.
‡Research Assistant, Department of Mechanics.